Supplemental Information:
Ethylene Oxide Monitor with Part-per-Trillion Precision for In-Situ Measurements

Tara I. Yacovitch, Christoph Dyroff, Joseph R. Roscioli, Conner Daube, J. Barry McManus, Scott C. Herndon

Aerodyne Research, Inc. Billerica MA, 01821 USA

Correspondence to: Tara I. Yacovitch (tyacovitch@aerodyne.com)

Table of Contents

S1 Instrument

S1.1 Optical setup of single-laser dual with 413 m cell

The basis of our EtO monitor is our commercially available (Aerodyne Research Inc., 2022a, b) dual-laser tunable infrared direct absorption spectrometer (TILDAS-FD) platform, which in this case is equipped with a single mid-infrared interband-cascade laser (nanoplus GmbH). The highly divergent beam of this laser is collected and focused into a long-pathlength multipass cell using a sequence of reflective optics (McManus et al., 2015). A visible laser is co-aligned using a dichroic mirror to aid the optical alignment of the system.

For the system described herein, we use a multipass cell with 413 m optical pathlength and an active volume of 1.8 litres for continuous flow applications. The cell contains two mirrors with wavelength-specific high-reflectivity coating (reflectivity >99.8%) to minimize reflective losses of laser power during the > 800 reflections among the two mirrors. Upon exiting the cell, the laser beam is focused on a thermoelectrically cooled photovoltaic HgCdTe detector (Judson, J19 with transimpedance amplifier).

The laser is driven by electrical current while being maintained at a constant temperature. The in-house software TDLWintel provides a voltage ramp via a digital-to-analogue converter card (National Instruments). This ramp is translated into current via a low-noise laser driver (QCL-500, Wavelength Electronics). The laser temperature is maintained by an electronic temperature controller via the built-in thermoelectric element in the sealed laser housing. The detector signal is digitized using an analogue-to-digital convert card (National Instruments) and then handled by TDLWintel for processing.

The laser wavelength is scanned across a narrow wavelength interval near 3065 cm-1 approximately 1830 times per second. For every scan, the laser is on for the first 90% of the time, followed by a brief period where it is off for the remaining 10% of the time. The individual spectra are then averaged to a single spectrum every 1 second. This averaged spectrum is then processed in TDLWintel to derive the mixing ratio of EtO as well as of all other absorbers defined in the spectroscopic fit at 1 Hz in real time.

Spectra are defined by absorption signal, a polynomial spectral baseline (full light, no absorption), as well as signal during the off period (no light, complete absorption). The latter two components are used to normalize the measured spectra onto the transmission scale (0 – 1).

The wavelength scale of the laser scan is determined by periodically analyzing the interference spectrum of a Germanium etalon. The derived wavelength scale is then further refined measuring a high-concentration ethylene (C_2H_4) spectrum from a reference cell built into an optional beam path in the spectrometer optics. Wavelength drift is mitigated by locking the laser to a strong H_2O line in the sample spectrum using an active feedback loop controller realized in software.

S1.2 Flow system

Sample gas is drawn through the multipass cell at a reduced pressure of 20 Torr (27 hPa) using a vacuum pump downstream of the instrument and an upstream pressure controller. This reduced pressure is used to sharpen the absorption lines in the

spectrum and provide the best compromise of spectroscopic selectivity and sensitivity. The gas-flow rate is typically around 3 – 5 slpm (slpm: standard litres per minute), resulting is a gas exchange rate of 1 Hz or better.

An overblow port is set up to deliver calibration gas or ultra-zero air. To prevent pressure disruptions, this port is tied into the inlet ~6 inches from the tip using a union tee. For humidity-matched zeroes, a parallel flow path is set up, with a length-matched piece of tubing and 6" by 1" scrubber cartridge isolated by two solenoid valves. We use a manganese dioxide/copper oxide catalyst as scrubber: Carulite 500® (Carus LLC), heated to 150 C. These valves actuate at the same time, pulling ambient air through the scrubber and providing near-humidity-matched zero air free of EtO.

Spectral backgrounding (or autobackgrounding) is done by intermittently and regularly measuring air free of EtO. A background spectrum is acquired and used to divide subsequent sample spectra, reducing the impact of drift due to instrumental effects like optical fringes and spectral baseline effects. Each background takes about 1 minute at 3 - 5 SLPM in order to flush out the cell, acquire clean spectra, and return to sampling.

S2 Calibration

The EtO-TILDAS instruments reports dry air mixing ratios that have been mathematically corrected for the dilution effects of water vapor, as well as for empirical water broadening effects. At the ambient humidity measured, these effects are expected to be < 3%.

In a typical calibration, 50-500 sccm of an EtO standard at 1 ppm EtO is delivered via an Alicat mass flow controller to a ½" overblow line connected via a T-fitting 6 inches from the inlet tip. Calibrations are done either by standard addition to humid ambient air, with a known total inlet flow rate (3 – 10 SLPM) or via dilution into a known flow (3-10 SLPM) of ultra-zero air delivered by a second Alicat mass flow controller. Humid standard additions are preferred, as they most closely resemble sampling conditions.

Standard concentrations were calculated based on the known calibration tank concentrations and the known system flows. Calibration factors (m) consist of the slope of a linear plot of measured EtO vs standard EtO, where true_conc = *m* * meas_conc.; when applying these calibration factors, divide the raw reported EtO by the slope. Two example calibration curves are shown below. Note that during dry calibrations in UZA, the EtO intercept is fixed to 0; during standard additions it is floated to account for potential ppt-level background concentrations. Example calibration curves for a dry (left) and humid (right) calibration are shown below. The 2021 Airgas calibration tank used in these results is shown in Figure S2

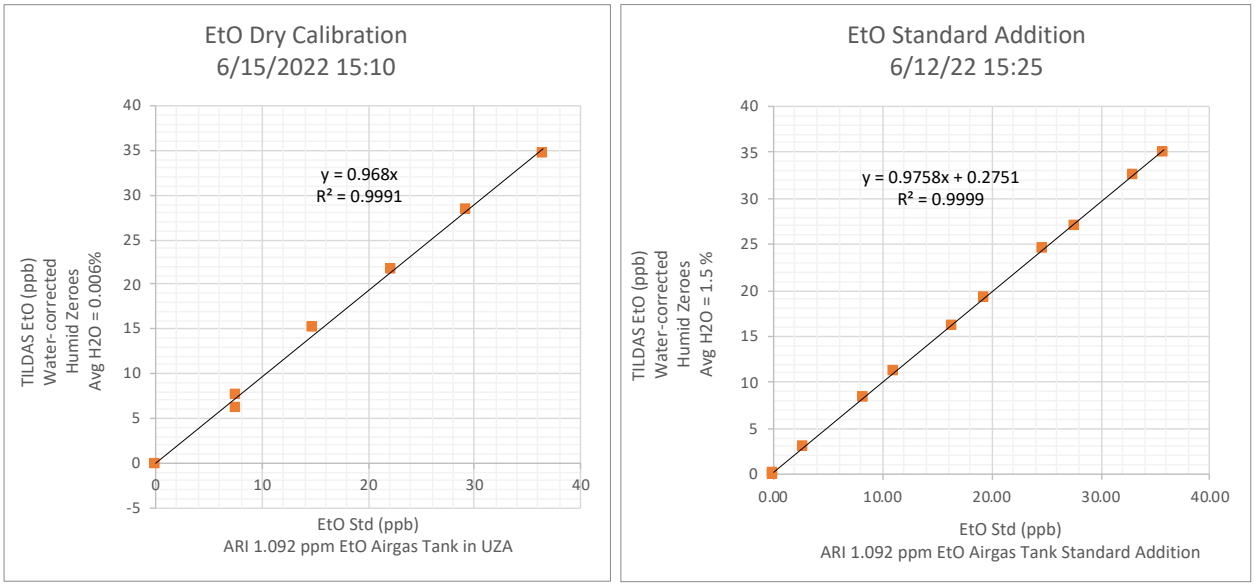

Figure S1. Example dry dilution (left) and standard addition (right) calibrations for EtO.

Airgas
an Air Liquide company

Airgas Specialty Gases
Airgas USA, LLC
6141 Easton Road
Bldg 1
Plumsteadville, PA 18949
Airgas.com

CERTIFICATE OF ANALYSIS

Grade of Product: CERTIFIED STANDARD-SPEC

Part Number:	X03NI99C15A05D3	Reference Number:	160-401988504-1
Cylinder Number:	CC68617	Cylinder Volume:	144.3 CF
Laboratory:	124 - Plumsteadville - PA	Cylinder Pressure:	2015 PSIG
Analysis Date:	Dec 31, 2020	Valve Outlet:	350SS
Lot Number:	160-401988504-1		

Product composition verified by direct comparison to calibration standards traceable to N.I.S.T. weights and/or N.I.S.T. Gas Mixture reference materials.

ANALYTICAL RESULTS

Component	Req Conc	Actual Concentration (Mole %)	Analytical Uncertainty
ETHANE	1.000 PPM	1.075 PPM	+/- 5%
ETHYLENE OXIDE	1.000 PPM	1.092 PPM	+/- 5%
NITROGEN	Balance		

Approved for Release

Page 1 of 160-401988504-1

Figure S2. Airgas calibration tank containing ethane and ethylene oxide at 1 ppm.

Table S1. Summary calibration factors for humid vs dry calibrations of ARI's Airgas tank X03NI99C15A05D3 over a week-long period

Statistics	Humid Standard Additions	Dry Calibrations
Average	0.981	0.999
StdDev	0.014	0.021
95% error	0.045	0.068
% error	4.6%	6.8%
1 ppb EtO would be corrected to	1.020	1.001

Table S2. Summary calibration factors for all calibrations of ARI's Airgas tank X03NI99C15A05D3 (both humid and dry) over a week-long period

Statistics	Average all ARI Tank
Average	0.979
StdDev	0.037
Count	9
95% error	0.084
% error	8.6%
1 ppb EtO would be corrected to	1.021
Certified Tank Conc (ppm)	1.092 ± 5%
Measured Tank Conc (ppm)	1.069 ± 8.6%

S3 Ambient Measurements

S3.1 Statistics for Ambient Measurements

Averages of the full time series, and of winter/spring (Feb 2022 – April 30 2022) and summer (July 1, 2022 – Aug 4, 2022) averages of the 1hr data shown in Figure 3 of the Manuscript are listed in Table S3 below. To understand whether the Winter/Spring and summer averages are significantly different, we compute the standard error of the mean (SEM), where SEM = SD/sqrt(N). We also include and propagate through a 5% error due to calibration uncertainty, yielding propagated error bars of 1-2 ppt for the averages. The upper and lower confidence limits at 95% confidence (UL and LL) are listed for winter/spring

and summer averages. The winter UL of 14 ppt does not overlap the summer LL of 31 ppt, leading us to conclude, using these Gaussian statistics, that the averages are significantly different at the 95% confidence level.

Since these statistics do include the small number of plumes observed, we also show histograms and Gaussian fits of the data in Figure S3. The Gaussian peaks occur at 12 ppt for the winter/spring and 32 ppt for summer, comparing well to the full averages computed in Table S3 of 12 ppt and 33 ppt, respectively, and do not alter the conclusions.

Table S3. Averages and statistics for 1hr ambient data shown in Figure 3 of the Manuscript, all values in ppb. "Winter/Spring" spans from February to April 30, 2022. "Summer" spans July to August 4, 2022. The standard Deviation (SD), number of 1hr averages (N), Student's T statistic at 95% confidence (t), 95% error bars using the SD are listed. Additional statistics for the mean are included: the standard error of the mean (SEM), 95% error bars for the average using the SEM, estimated error bars assuming a 5% calibration uncertainty, the resulting propagated error, and the resulting 95% Lower Limit (LL) and Upper Limit (UL) for winter and summer averages.

	Avg	SD	N	t, 95% Conf	95% Error using SD	SEM	95% error from SEM	Error 5% Cal. Uncert	Prop-agated error	LL	UL
All Data shown in Manuscript Figure 3 Error! Reference source not found.	0.018	0.022	2610	1.961	0.043	0.0004	0.0008	0.001	0.001	0.017	0.020
Winter/ Spring (ending 30 April)	0.012	0.023	1613	1.961	0.044	0.0006	0.0011	0.001	0.001	0.011	0.014
Summer (beginning 1 July)	0.033	0.013	485	1.965	0.026	0.0006	0.0012	0.002	0.002	0.031	0.035

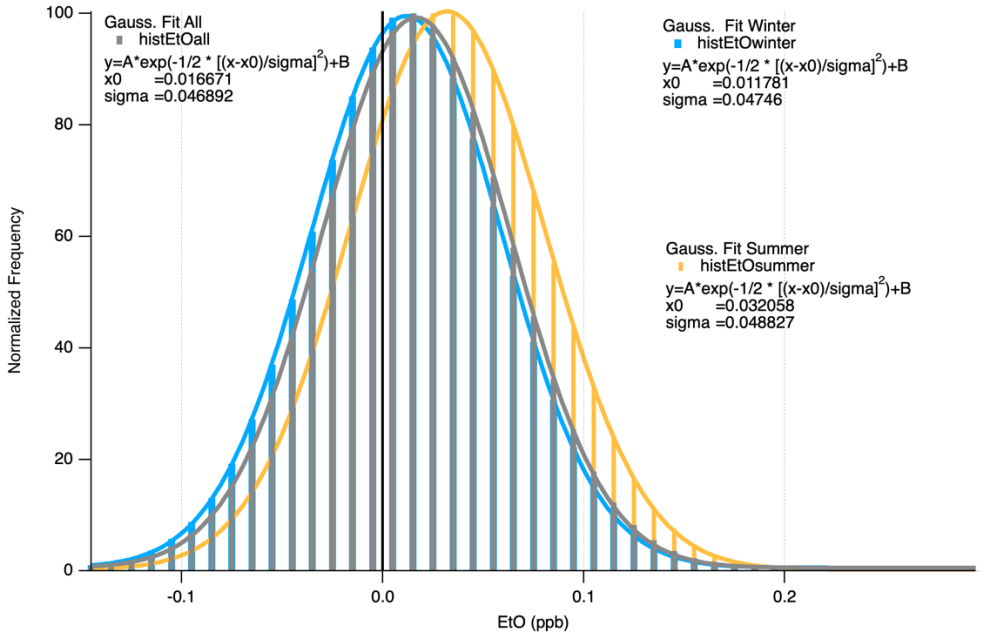

Figure S3. Histogram of 1hr average data in winter/spring (blue), summer (yellow) and all ambient measurements (grey).

S3.2 Hysplit Back Trajectories

The back trajectory analysis was computed using the National Oceanic and Atmospheric Administration (NOAA) Air Resources Laboratory (ARL) Hybrid Single-Particle Lagrangian Integrated Trajectory model (HYSPLIT). The work depicted here in the SI used the web-based model with default options. The parameters for the run are noted in the figure legend. This work involved straightforward back trajectory calculation. Although HYSPLIT is capable of a rigorous source-receptor analysis, the physical correspondence noted below has been performed 'by eye', not via a quantitative attribution. Details of the NOAA/ARL HYSPLIT model (Rolph et al., 2017; Stein et al., 2015) can be found in the cited sources or at the primary website (https://www.arl.noaa.gov/hysplit/).

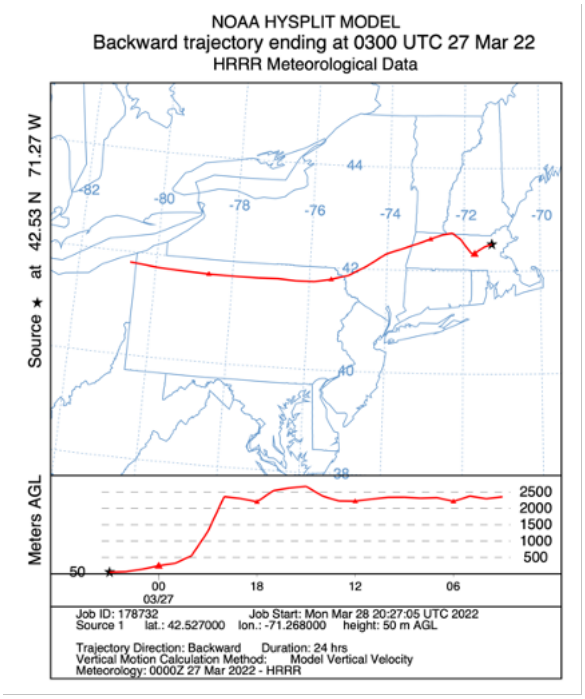

Figure S4. Back trajectory simulation for the EtO event on 3/27/2022. (NOAA Air Resources Laboratory)

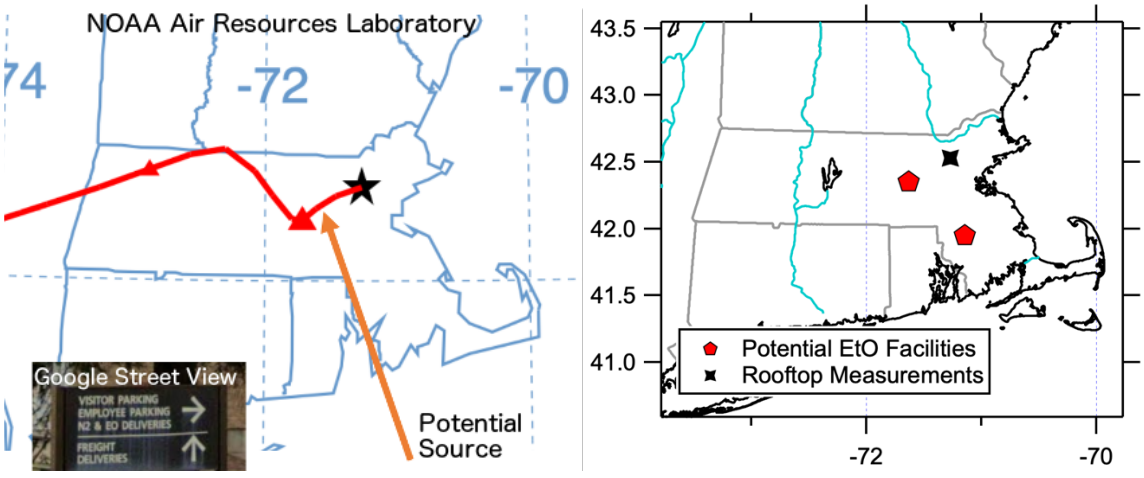

Figure S5. Left: Detail of back trajectory (NOAA Air Resources Laboratory). The orange arrow indicates location of one potential EtO source in the state. A roadside-view of this facility's signage is inset (© Google Street View), with "EO deliveries" noted. Right: Location of rooftop measurements (black marker) and two potential EtO facilities (red markers) in the state of Massachusetts. Map outlines from NOAA (NOAA, 2013).

S4. Mobile Measurements

S4.1 Facility A measurements

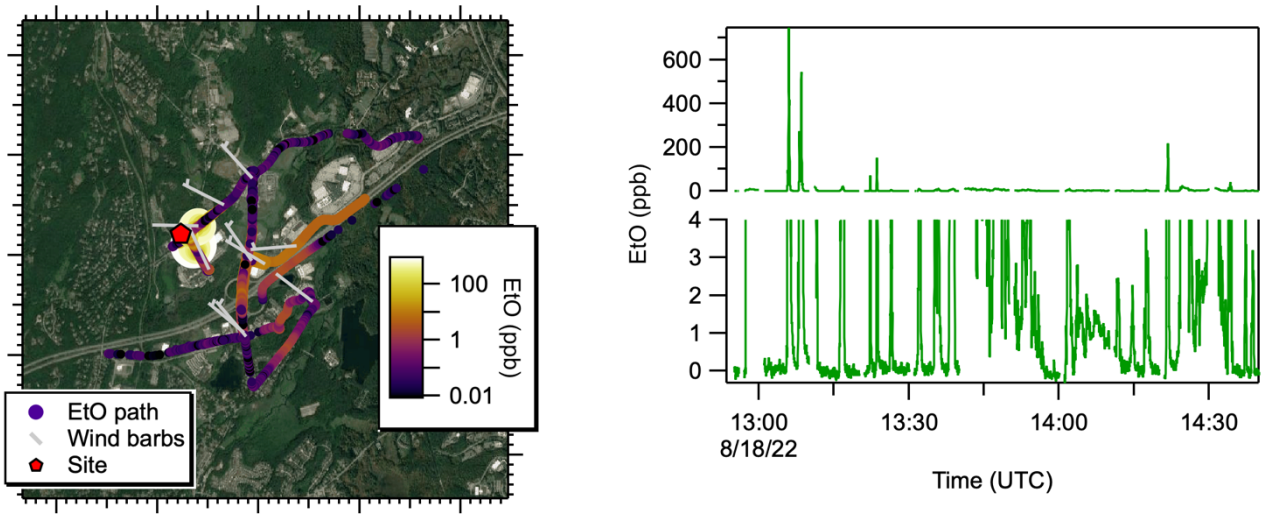

Figure S6. Morning summary data downwind of Facility A. A map (left) shows AML path colored by EtO concentration, with wind barbs tethered to the truck path, and feather end of the staff pointing into the wind. Time series show EtO concentrations zoomed to 0-4 ppb (bottom right) and at full scale (top right). Map underlay: Google, © 2022 CNES / Airbus, Landsat / Copernicus, MassGIS, Commonwealth of Massachusetts EOEA, Maxar Technologies, USDA/FPAC/GEO

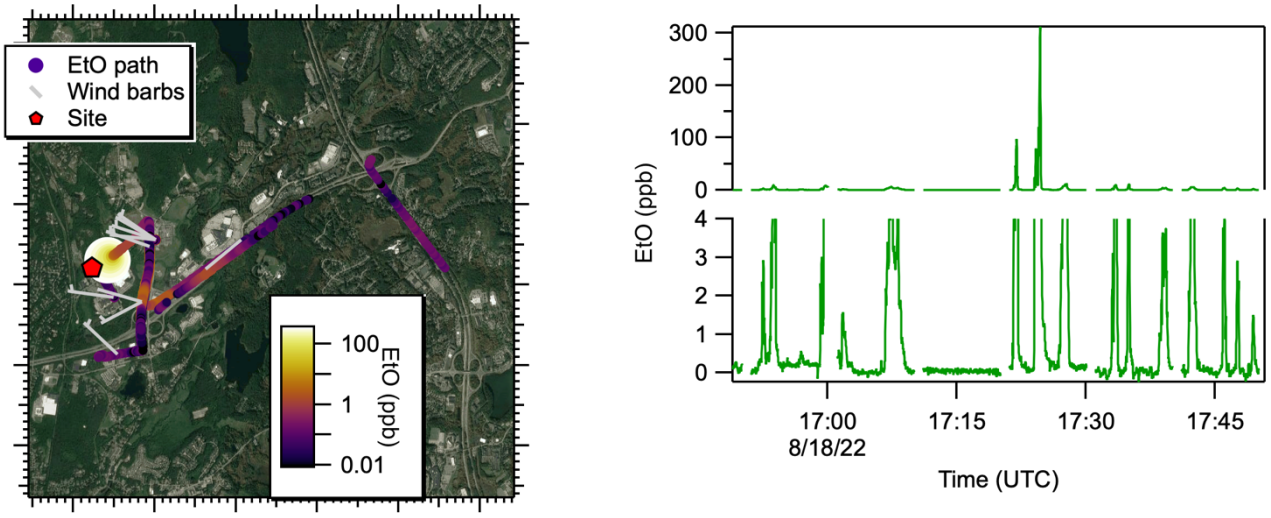

Figure S7. Afternoon Summary data downwind of Facility A. A map (left) shows AML path colored by EtO concentration, with wind barbs pointing into the wind. Time series show EtO concentrations zoomed to 0-4 ppb (bottom right) and at full scale (top right). Map underlay: Google, © 2022 CNES / Airbus, Landsat / Copernicus, MassGIS, Commonwealth of Massachusetts EOEA, Maxar Technologies, USDA/FPAC/GEO

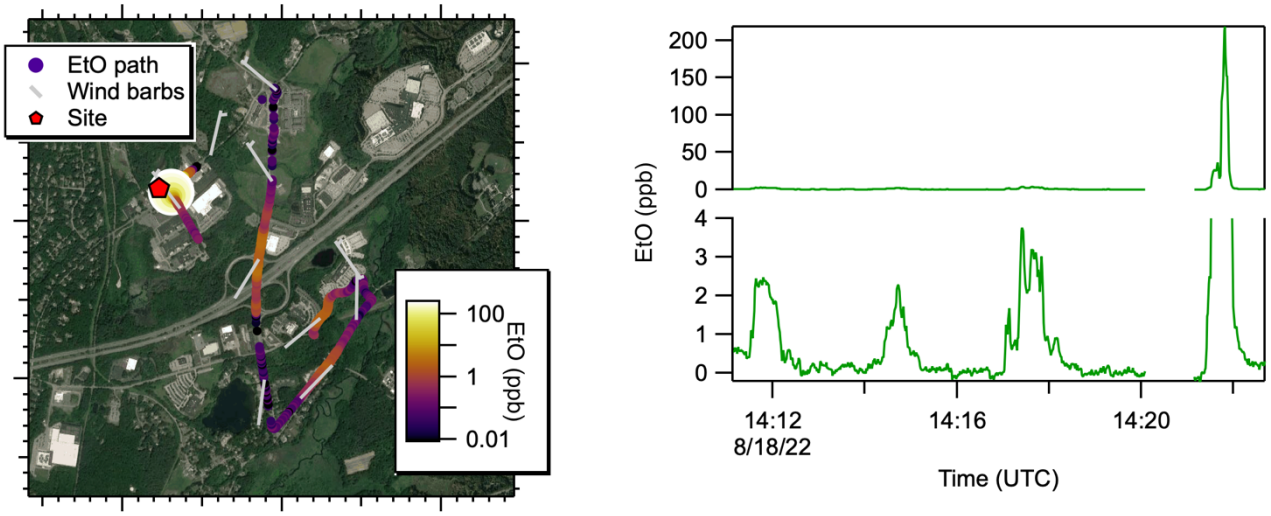

Figure S8. Detail of Morning Transect Downwind of Facility A. A map (left) shows AML path colored by EtO concentration (log scale), with wind barbs tethered to the truck path, and feather end of the staff pointing into the wind. Time series show EtO concentrations zoomed to 0-4 ppb (bottom right) and at full scale (top right). Map underlay: Google, © 2022 CNES / Airbus, Landsat / Copernicus, MassGIS, Commonwealth of Massachusetts EOEA, Maxar Technologies, USDA/FPAC/GEO

Spatial averaging was done for all data collected on 8/18/2022 at Facility A. Bins are 100m x 100m in size.

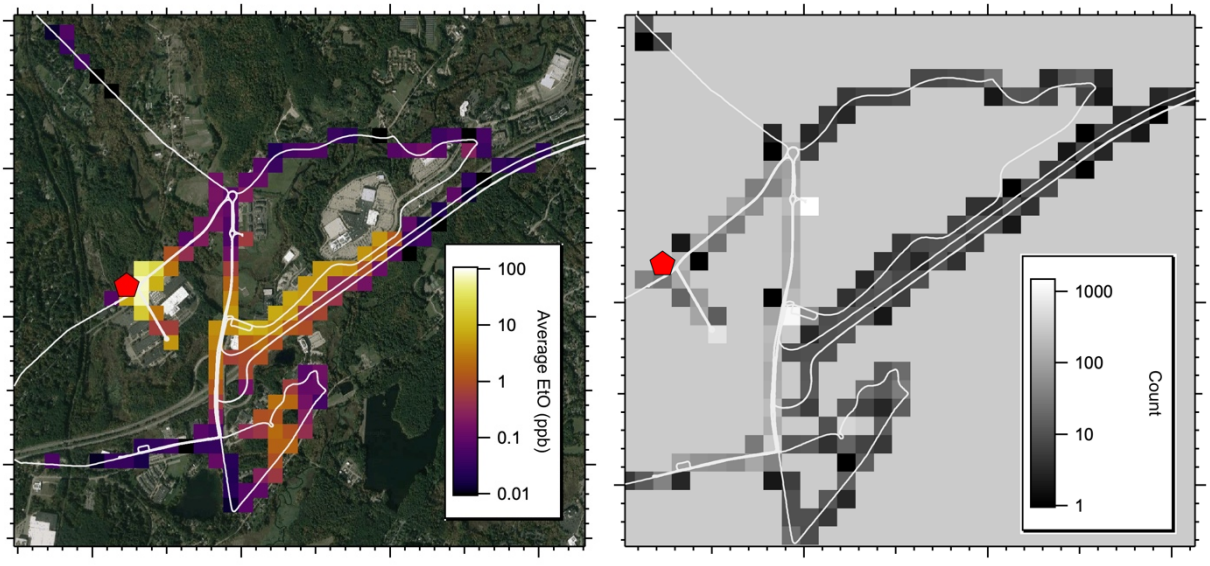

Figure S9. Binned average EtO concentrations (log scale) downwind of Facility A (left) along with data point count (right). The facility is located at the red marker. Wind was consistently from the North-West during these measurements. Map underlay: Google, © 2022 CNES / Airbus, Landsat / Copernicus, MassGIS, Commonwealth of Massachusetts EOEA, Maxar Technologies, USDA/FPAC/GEO

The archived spectra can be used to unambiguously spectrally fingerprint the EtO observed at these facilities. For example, Figure S10 (top) shows raw measured signal out of plume (black) overlaid on signal in-plume (gold area) at Facility A. In Figure S10 (bottom), we manually divide the in-plume and out-of-plume spectra to reveal the spectral signature of EtO. Line scars at the positions of the water lines are observable (green spikes) due to slight variations in laser peak position. The blue line is a transmission simulation of EtO only, and clearly matches the experimental result.

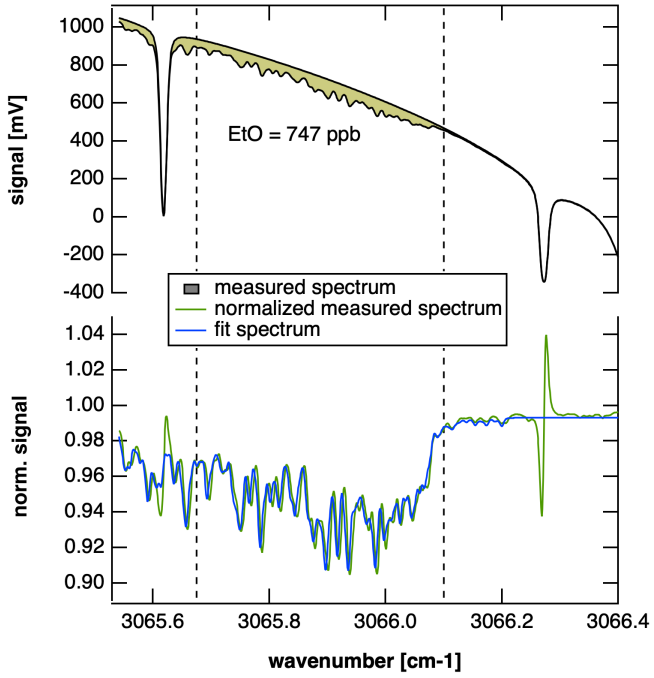

Figure S10. Summary spectra comparing instantaneous Facility A measurement of 747 ppb (in-plume, gold) to an out-of plume spectrum. The top shows signal as a function of wavenumber, with EtO contributions highlighted in yellow. The bottom shows a divided spectra in-plume/out-of-plume (green) and transmission simulation of EtO only.

S4.2 Facility B Measurements

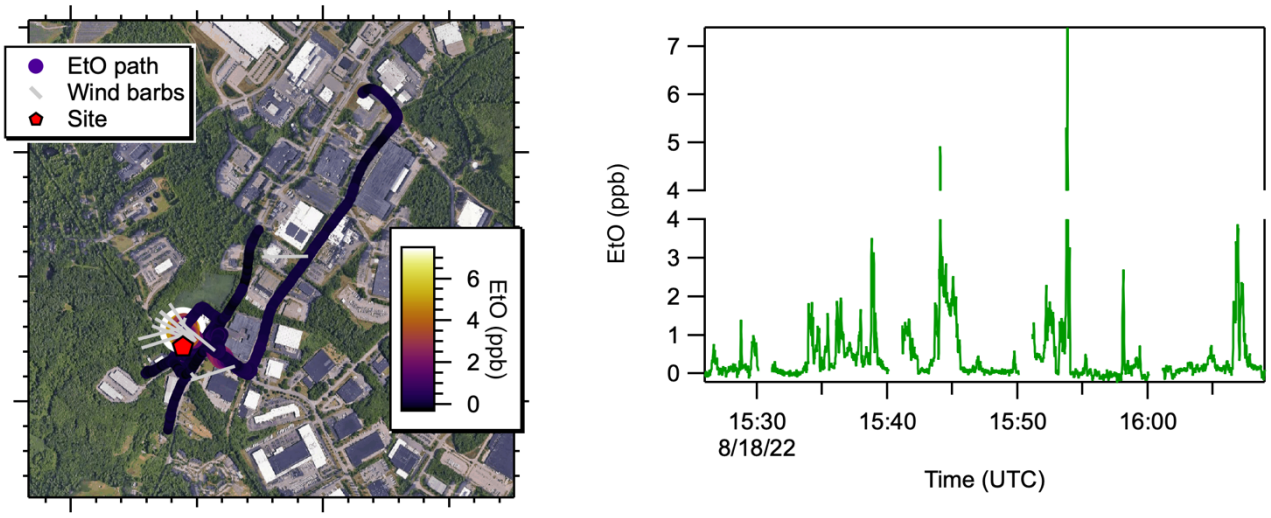

Figure S11. Full Summary time series downwind of Facility B. A map (left) shows AML path colored by EtO concentration, with wind barbs tethered to the truck path, and feather end of the staff pointing into the wind. Time series show EtO concentrations zoomed to 0-4 ppb (bottom right) and at full scale (top right). Map underlay: Google, © 2022 CNES / Airbus, Landsat / Copernicus, MassGIS, Commonwealth of Massachusetts EOEA, Maxar Technologies, RIGIS, USDA/FPAC/GEO

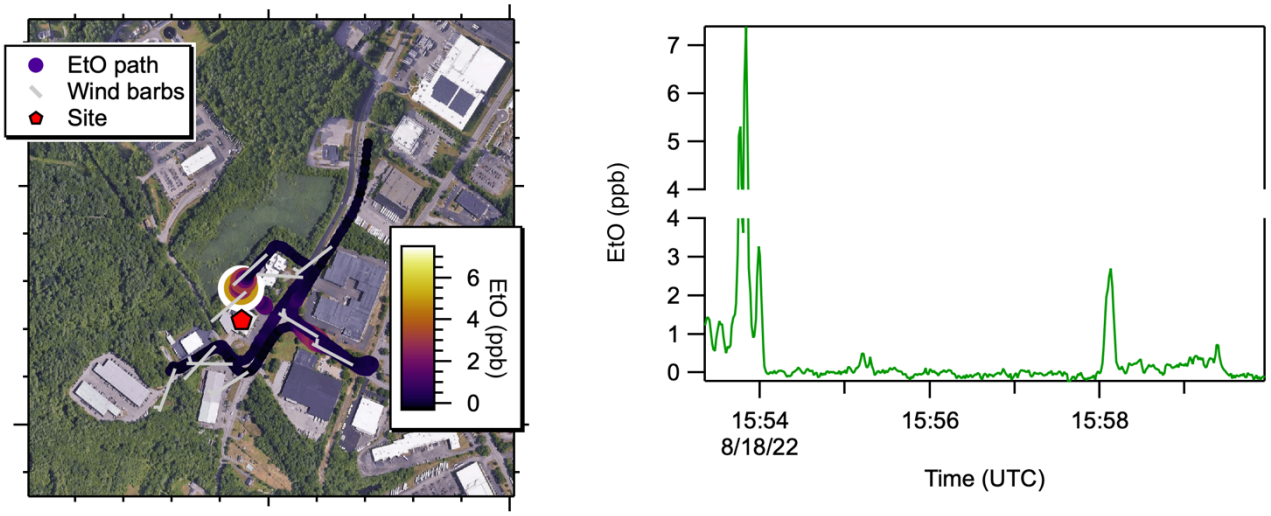

Figure S12. Detail of time series downwind of Facility B. A map (left) shows AML path colored by EtO concentration, with wind barbs tethered to the truck path, and feather end of the staff pointing into the wind. Time series show EtO concentrations zoomed to 0-4 ppb (bottom right) and at full scale (top right). Map underlay: Google, © 2022 CNES / Airbus, MassGIS, Commonwealth of Massachusetts EOEA, Maxar Technologies, RIGIS, USDA/FPAC/GEO

Spatial averaging was done for all data collected on 8/18/2022 at Facility B. Bins are 100m x 100m in size.

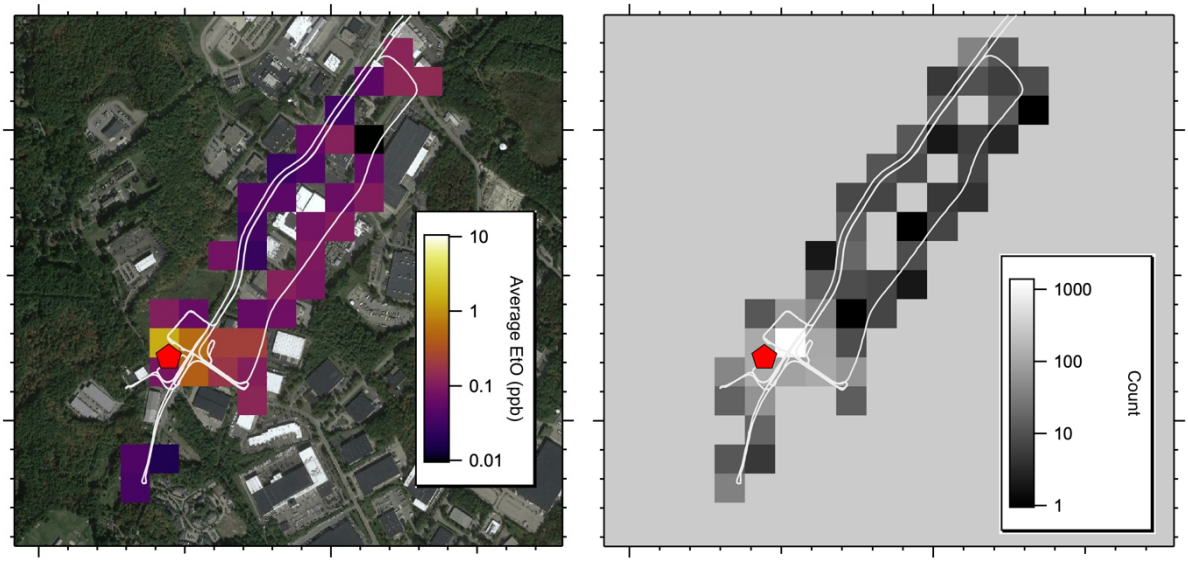

Figure S13. Binned average EtO concentrations downwind of Facility B (left) along with data point count (right). The facility is located at the red marker. Wind was from the West during these measurements. Map underlay: Google, © 2022 CNES / Airbus, MassGIS, Commonwealth of Massachusetts EOEA, Maxar Technologies, RIGIS, USDA/FPAC/GEO

References

Aerodyne Research Inc.: Laser trace gas and isotope analyzers, 2022a. https://www.aerodyne.com/product/laser-trace-gas-and-isotope-analyzers/, last

Aerodyne Research Inc.: TILDAS compact single laser ethylene oxide analyzer, 2022b. https://www.aerodyne.com/wp-content/uploads/2022/01/EthyleneOxide.pdf, last

McManus, J. B., Zahniser, M. S., Nelson, D. D., Shorter, J. H., Herndon, S. C., Jervis, D., Agnese, M., McGovern, R., Yacovitch, T. I., and Roscioli, J. R.: Recent progress in laser-based trace gas instruments: Performance and noise analysis, Applied Physics B, 119, 203-218, 10.1007/s00340-015-6033-0, 2015.

NOAA: Global self-consistent, hierarchical, high-resolution geography database (GSHHG): Version 2.2.0, 2013.

Rolph, G., Stein, A., and Stunder, B.: Real-time environmental applications and display system: Ready, Environmental Modelling & Software, 95, 210-228, https://doi.org/10.1016/j.envsoft.2017.06.025, 2017.

Stein, A. F., Draxler, R. R., Rolph, G. D., Stunder, B. J. B., Cohen, M. D., and Ngan, F.: NOAA's HYSPLIT atmospheric transport and dispersion modeling system, Bulletin of the American Meteorological Society, 96, 2059-2077, 10.1175/bams-d-14-00110.1, 2015.